The Ordering of Ordinary Moiré Fringes by Photometric Analysis

Ding Xinhong[†] and J. R. Pekelsky

Division of Physics
National Research Council of Canada
Ottawa, Canada. K1A 0R6

Abstract

Ordinary moiré is characterized by a fixed pattern of fringes that are symmetric with respect to the sign of the surface gradient. One cannot distinguish from such fringes alone whether a fringe (contour) lies above or below its neighbour. Known as the "hill-or-valley" dilemma, this ambiguity has been cited as the principal weakness of ordinary moiré topograms. The 'up' or 'down' surface orientation possiblities generally result in sufficiently different surface reflectance such that only one is consistent with the values measured in the topogram. The photometric model used to predict the expected surface brightness is based upon the relative position of the source, the object surface and the camera, as well as the local surface reflectance properties. The theoretical and practical constraints of this method are discussed, and analyzed topograms of test objects and human subjects serve to illustrate the principle of photometric fringe ordering.

1. Introduction

Moiré fringes are produced by using the moiré effect on the surface of an object. Under suitable conditions, these fringes can be designed to represent the contours of the surface from which one can derive 3–D information of the object. One of the basic unsolved problems in moiré fringe analysis is the ordering of ordinary moiré fringes. *Ordinary* moiré fringes are those which are both fixed-encoded and grade-symmetric (Pekelsky, 1985). One cannot distinguish from such fringes alone whether a fringe (contour) lies above or below its neighbour. This ambiguity has been cited as the principal weakness of ordinary moiré topograms. Hybrid moiré techniques circumvent this issue in various fashions (Pekelsky, 1985), but motivated by the inherent simplicity of the ordinary moiré method and its potentially broad range of application, we have sought a general solution to the problem. The approach described here is related to the so-called *shape-from-shading* technique in computer vision, which has inspired extensive works during recent years (Horn, 1975).

In the shape-from-shading technique, the main purpose is to derive 3–D information from the 2–D image. The basic idea in this technique is to use photometric modeling to connect the image intensity with the surface orientation of the object so that it is possible to derive a consistent net of 3–D surface coordinates from a 2–D distribution of image intensities. The general approach in this method combines an image formation model and a reflectance function (plus some smoothness constraints) for the surface to select the object's shape from an infinite set of possibilities (Ikeuchi and Horn, 1981). Moiré fringe ordering is a 2–D to 3–D problem of a much simpler class: a great deal of topographic information is known *a priori* in that the projections of the surface contours

[†] Visiting Scientist from the Nanjing Research Institute of Electronic Engineering, P.O. Box 1406, Nanjing, P.R.C.

(the moiré fringes) are known and thus the set of shapes from which to choose is quite small. It is this reduction from a continuum to a few discrete choices that suggest it may be possible to order ordinary moiré fringes by using photometric analysis, as was first proposed in an earlier article (Pekelsky, 1984). In this study we continue to use the principles of central projection geometry and a simple reflectance function to predict the reflectance value at given point on a contour for each valid fringe order relationship and to then choose that order relationship which produces the least squared error between the measured reflectance value and the predicted reflectance value.

In Section 2 we describe the moiré image formation geometry for our case, and define the scope of the fringe ordering problem. In Section 3 we present the photometric model used in this paper and the concept of ordering the fringes using photometric knowledge. The evaluation of the local surface normal is central to our analysis, and in Section 4 we develop an algorithm to estimate the surface normal at given point. In Section 5 we describe the basic steps of our fringe ordering method and in Section 6 some preliminary experiment results are presented.

2. Moiré Image Formation Geometry and Fringe Ordering

Figure 1 illustrates the moiré image formation geometry, which can be recognized as a classical two-projection-center photogrammetric arrangement. We use $(\mathbf{X}, \mathbf{Y}, \mathbf{Z})$ to denote the 3-D Cartesian coordinate system, where the $(\mathbf{X}, \mathbf{Y})$ plane is the grid plane of the moiré instrument and consists of a frame supporting parallel strings separated by a distance d from one another. In front of the grid plane there is a light source at the first projection center, with coordinate $(0, h, l)$. The light shines through the strings, and onto an object placed behind the grid plane, thus encoding it with stripes of light characterizing the position of that projection center. The **Z**-axis points to the viewer (camera) position at the second projection center, which has coordinate $(0, 0, l)$. The scene thus viewed by the camera consists of the grid pattern and the (distorted but similar) projected stripe pattern superimposed to form the "moiré", which is recorded on film in the $(\mathbf{U}, \mathbf{V})$ plane.

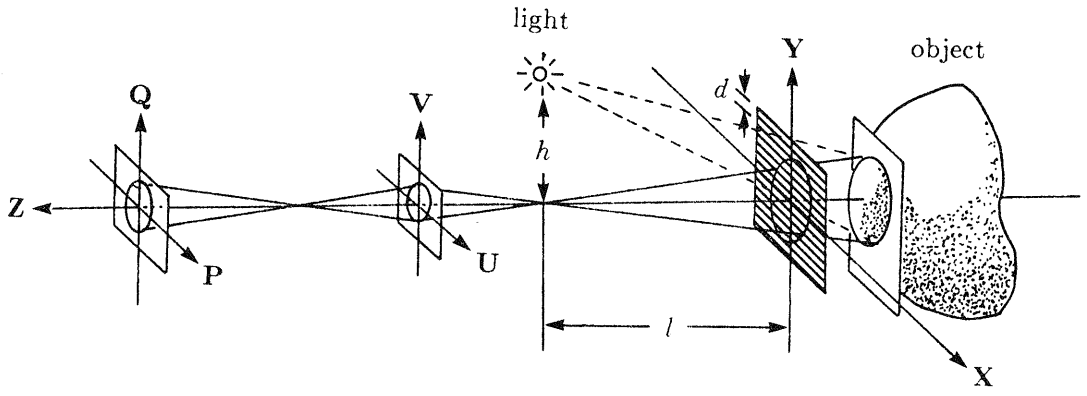

Figure 1. The Moiré Geometry

In a subsequent step, a scanner is used to transform this moiré *topogram* into a digital image in the $(\mathbf{P}, \mathbf{Q})$ image plane, and the *topographic contours* are delineated (automatically or by hand) by tracing the loci of moiré fringe intensity extrema (the *bright* and/or *dark* moiré fringes) in the image plane. These loci are indeed fringe-encoded contours by virtue of moiré geometry used (Van Wijk, 1980).

Let $F(t) = (p(t), q(t))$ and $G(t) = (x(t,0), y(t,0))$ be the parametric equation representations of the moiré fringes on the $(\mathbf{P}, \mathbf{Q})$ and $(\mathbf{X}, \mathbf{Y})$ planes respectively. Let $C(t,n) = (x(t,n), y(t,n), z(n))$ be the corresponding parametric equation representation of the contour in the $(\mathbf{X}, \mathbf{Y}, \mathbf{Z})$ space, where t is the curve parameter and $0 \leq n < h/d$ is the fringe number, an index for the contour plane ($n = 0$ corresponds to the grid plane). Then:

$$x(t,0) = a_{11}p(t) + a_{12}q(t) + a_{13}, \tag{1a}$$

$$y(t,0) = a_{21}p(t) + a_{22}q(t) + a_{23}, \tag{1b}$$

$$x(t,n) = (1 - \frac{nd}{nd-h})x(t,0), \tag{2a}$$

$$y(t,n) = (1 - \frac{nd}{nd-h})y(t,0), \tag{2b}$$

$$z(n) = \frac{ndl}{nd-h}. \tag{3}$$

Equation 1 is the affine transformation for a point (p,q) in the image plane to a point (x_g, y_g) in the grid plane, and coefficients a_{ij} are determined by image registration using known control points. Equation 2 provides a central projection into object space with scale corrections provided by Eq. 3, the moiré fringe elevation formula. Equations 1–3 map the *plane curve* (a moiré fringe) in the $(\mathbf{P}, \mathbf{Q})$ image plane to the corresponding *space curve* (a surface contour) in the $(\mathbf{X}, \mathbf{Y}, \mathbf{Z})$ object space.

Consider a moiré topogram with M *bright* [1] fringes $F_1, F_2, \ldots, F_M$. Let $n_1, n_2, \ldots, n_M$ be their corresponding fringe numbers and $C_1, C_2, \ldots, C_M$ are the corresponding contours of these fringes. Then the fringe ordering problem can be stated as: given M fringes $F_1, F_2, \ldots, F_M$, determine whether contour C_i is at a lower, equal or higher elevation than contour C_j for each $i, j = 1, 2, \ldots, M$. Since the contour elevation $z(n)$ is a monotonic function of the fringe number n (Eq. 3), therefore the moiré fringe ordering problem can be equivalently stated as: determine for M fringes $F_1, F_2, \ldots, F_M$ whether $n_j < n_i$, $n_j = n_i$ or $n_j > n_i$ for each $i, j = 1, 2, \ldots, M$. For the convenience of the subsequent discussions we use $n_j \Omega n_i$ to denote an order relationship between fringes F_j and F_i, where $\Omega \in \{<, =, >\}$ is an order symbol.

Without any loss of generality, it is sufficient to determine the relationship only between *neighbouring fringes*. If F_i and F_j are two neighbouring fringes then according to the axiomatic definition of a *contour*, their fringe numbers can differ by at most one contour interval, i.e.

$$n_j = \begin{cases} n_i - 1, & \text{if } \Omega \text{ is } < \ ; \\ n_i, & \text{if } \Omega \text{ is } = \ ; \\ n_i + 1, & \text{if } \Omega \text{ is } > \ . \end{cases} \tag{4}$$

Let F denote the *dark* fringe that lies between F_i and F_j and m denote its fringe number. Clearly, F must be either a half-interval *above* or *below* F_i, and it follows that

$$m = \begin{cases} n_i - 1/2, & \text{if } \Omega \text{ is } < \ ; \\ n_i \pm 1/2, & \text{if } \Omega \text{ is } = \ ; \\ n_i + 1/2, & \text{if } \Omega \text{ is } > \ . \end{cases} \tag{5}$$

Note that when F_i and F_j are at the same elevation, m will have two possible values and thus there are four cases of the n_i, n_j and m combinations to consider.

[1] Alternately, we could use the dark fringes in this discussion, indeed we use them in our tests.

3. The Photometric Model

The possibility of using photometric knowledge to solve the fringe ordering problem is founded on the premise that the image brightness contains 3–D information. In order to use this information to determine the order relations between neighbouring fringes, we first need a photometric model and a reflectance function that will allow image brightness to be related directly to surface orientation. We must then derive a way that can relate the orientation to the order relationship Ω between two neighbouring fringes. The simplest photometric situation is that of a single point-source as shown in Fig. 2, where the geometry of the reflected light is governed by three vectors: the illumination direction L, the surface normal N and the viewer's direction V (Pentland, 1984). If we further assume a Lambert (i.e. purely diffuse) surface, then the reflectance funtion at any given point on the surface can be written as:

$$I = \rho\lambda\frac{(N \cdot L)}{r^2} = I_0\frac{(N \cdot L)}{r^2} \tag{6}$$

where I is the reflectance value, ρ is the albedo of the surface, λ is the nominal intensity of the light source, r is the distance to the light source and $N \cdot L$ is the inner product. For simplicity we use I_0 as a single parameter to replace $\rho\lambda$ in the formula. This is a model for a purely diffuse surface under finite-distance single-point illumination.

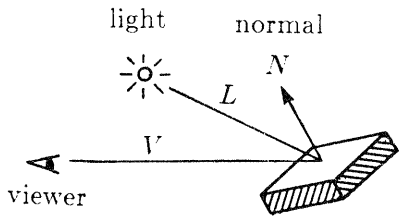

Figure 2. The Geometry of the Photometric Model

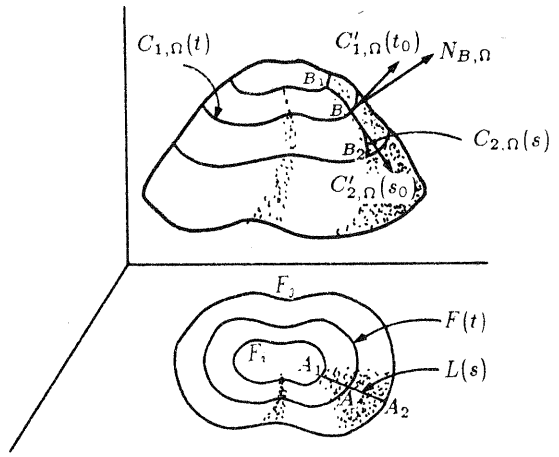

Figure 3. The Determination of the Surface Normal

For each different order relationship $n_j \Omega n_i$ between two neighbouring fringes, the corresponding contours on the surface of the object will be at different elevations due to the different n_j, n_i and m value combinations (Eqs. 4–5). This specifies different surface orientations that will, in general, produce different reflectance values according to the photometric model. By comparing these reflectance values with the image brightness we would expect that only the reflectance value produced due to the correct order relationship assumption will be most consistent with the image brightness. This is the underlying principle of the photometric ordering of moiré fringes.

To use this photometric model we must first obtain the model parameter I_0. In general, at different points of the surface I_0 will take different values. But when two points are close enough we would expect that the change in I_0 is small. Therefore we begin from a point P_1 where the value $(N \cdot L)/r^2$ is known and simply divide this value to the imge brightness to obtain the model parameter I_{0,P_1}. This parameter is then applied to a nearby point P_2 to calculate the reflectance value there for different surface orientation cases and to carry out the fringe ordering analysis. Once

the order relationship near P_2 has been determined, the correct orientation there will be used to obtain a model parameter I_{0,P_2} and this parameter will be used for the next nearby point, and so forth.

4. The Determination of the Surface Normal

One of the key problems in using the photometric model to estimate the reflectance values at a given point is the estimation of the surface normal at that point. In this section we develop an algorithm which can solve this problem for our case.

Referring to Fig. 3, let $F_i(t)$ and $F_j(t)$ be the parametric equation representations for the two neighbouring *bright* fringes F_i and F_j on the $(\mathbf{P},\mathbf{Q})$ image plane and $F(t) = \big(f_1(t), f_2(t)\big)$ be the parametric equation representation of *dark* fringe F between F_i and F_j. Let A be a given point on $F(t)$ and B the corresponding point on the surface of the object. Through point A is drawn a straight line segment $L(s) = \big(l_1(s), l_2(s)\big)$ which is orthogonal to the tangent vector of $F(t)$ at A and intersects $F_i(t)$, $F_j(t)$ at points A_1, A_2 respectively. We use B_1 and B_2 to denote the corresponding points on the surface for A_1 and A_2. Let n_i, n_j and m be the fringe numbers of F_i, F_j and F respectively, then from Eqs. 4–5, for each given order relationship between F_i and F_j, n_i, n_j and m take different values. Based on these values and the Eqs. 1–3, we can map the plane curves $F(t)$ and $L(t)$ to corresponding surface curves $C_{1,\Omega}(t)$ and $C_{2,\Omega}(s)$, where Ω indicates that these curves are order relationship dependent. According to Eqs. 1–3, $C_{1,\Omega}$ can be determined as:

$$\left.\begin{aligned} C_{1,\Omega}(t) &= \big(x_{1,\Omega}(t), y_{1,\Omega}(t), z_{1,\Omega}(t)\big), \\ x_{1,\Omega}(t) &= \big(1 - \frac{md}{md-h}\big)\big(a_{11}f_1(t) + a_{12}f_2(t) + a_{13}\big), \\ y_{1,\Omega}(t) &= \big(1 - \frac{md}{md-h}\big)\big(a_{21}f_1(t) + a_{22}f_2(t) + a_{23}\big), \\ z_{1,\Omega}(t) &= \frac{mdl}{md-h}. \end{aligned}\right\} \tag{7}$$

To determine $C_{2,\Omega}(s)$ we interpolate the function using the three known points B_1, B and B_2. Since $L(s)$ is a straight line, the components of $C_{2,\Omega}(s)$ in the **X**,**Y**-axes directions are linear functions of s. As to the component in the **Z**-axis direction, we simply use a quadratic function to interpolate it. Therefore we have

$$\left.\begin{aligned} C_{2,\Omega}(s) &= \big((x_{2,\Omega}(s), y_{2,\Omega}(s), z_{2,\Omega}(s)\big), \\ x_{2,\Omega}(s) &= \big(\alpha_{1,\Omega}s + \beta_{1,\Omega}\big), \\ y_{2,\Omega}(s) &= \big(\alpha_{2,\Omega}s + \beta_{2,\Omega}\big), \\ z_{2,\Omega}(s) &= \big(a_\Omega s^2 + b_\Omega s + c_\Omega\big), \end{aligned}\right\} \tag{8}$$

where the coefficients $\alpha_{1,\Omega}, \beta_{1,\Omega}, \alpha_{2,\Omega}, \beta_{2,\Omega}, a_\Omega, b_\Omega, c_\Omega$ are order relationship dependent, and can be determined from the components of B_1, B and B_2.

The local surface normal at point B is now simply the vector product of two tangent vectors $C'_{1,\Omega}(t)$ and $C'_{2,\Omega}(s)$ at that point (the corresponding curve parameters at this point are $t = t_0, s = s_0$):

$$N_{B,\Omega} = \frac{C'_{2,\Omega}(s_0) \times C'_{1,\Omega}(t_0)}{|C'_{2,\Omega}(s_0) \times C'_{1,\Omega}(t_0)|}, \tag{9}$$

where $'$ represents the derivative with respect to the parameter. Note that the surface normal $N_{B,\Omega}$ depends on both the order symbol Ω for the two neighbouring fringes $F_1(t)$ and $F_2(t)$ as well as the corresponding point B on the contour.

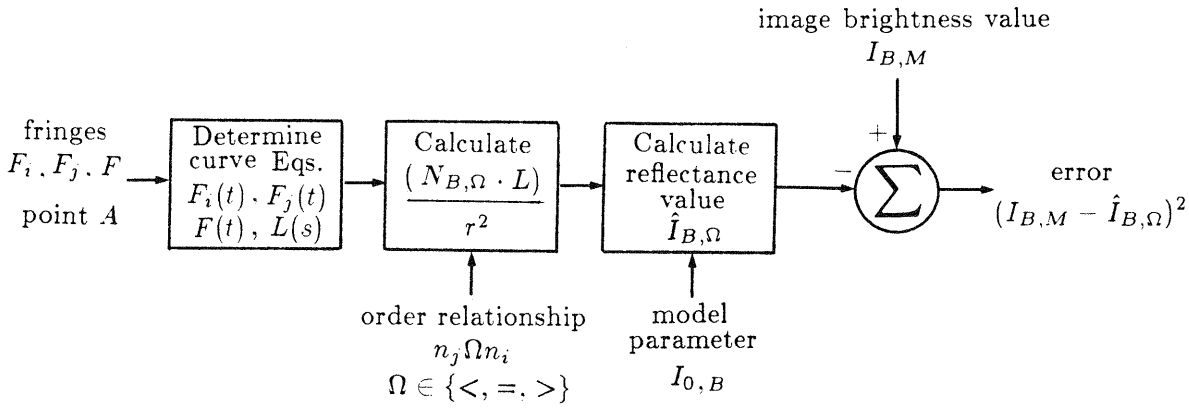

Figure 4. Block Diagram for Moiré Fringe Ordering Algorithm

5. The Fringe Ordering Algorithm

Based on the previous discussion regarding moiré image formation geometry, the photometric model and the determination of the surface normal, we now can present an algorithm for moiré fringe ordering. Assume that fringes F_h, F_i and F_j are a sequence of neighbouring fringes where F_h, F_i have been ordered, and now we want to determine the order relationship between fringes $F_i(t)$ and $F_j(t)$: $n_j \Omega n_i$. The process is specified below:

Step 1. Choose a point A on the fringe $F(t)$, where $F(t)$ is the dark fringe between $F_i(t)$ and $F_j(t)$.

Step 2. Determine plane curves equations $F(t)$ and $L(s)$, where $L(s)$ connects fringes F_i, F and F_j at points A_1, A and A_2 respectively (Fig. 3).

Step 3. For each order relationship $n_j \Omega n_i$, obtain the values n_i, n_j and m by using Eqs. 4–5. Based on these fringe numbers, find the corresponding points B, B_1 and B_2 of points A, A_1 and A_2. Then map the plane curves $F(t)$ and straight line segment $L(s)$ to the surface curves $C_{1,\Omega}(t)$ and $C_{2,\Omega}(s)$ by using Eqs. 7–8 and calculate the surface normal $N_{B,\Omega}$ (Eq. 9), the vector L and the inner product of these two vectors.

Step 4. Use the known fringes F_h, F_i to obtain an estimation of the model parameter I_0 in a point near point B and apply this parameter to point B.

Step 5. Calculate reflectance values $\hat{I}_{B,\Omega}$ for each Ω using the local photometric model (Eq. 6).

Step 6. For each order symbol Ω, calculate the error between the measured image brightness value $I_{B,M}$ and the estimated reflectance value $\hat{I}_{B,\Omega}$ and choose the order relationship $n_j \Omega n_i$ which produces the least square error. To make this method more reliable we can repeat the process for several points $A_1, A_2, \ldots, A_N$ (the corresponding points on the surface contour are $B_1, B_2, \ldots, B_N$) on the fringe $F(t)$ and make the final decision based on the total error. Therefore the order relation will be determined according to the following rule:

$$\min_{\Omega \in \{<,=,>\}} \sum_{B=B_1}^{B_N} (I_{B,M} - \hat{I}_{B,\Omega})^2. \tag{10}$$

Figure 4 illustrates the whole procedure. To start this algorithm an initial model parameter is

needed. One way to obtain it is by assuming that there are two neighbouring fringes whose fringe numbers are initially known. This is not a strict assumption because in most moiré topograms a fiducial string can be arranged to absolutely identify the fringe number of the fringes its shadow intersects (Takasaki, 1970). Then by using Eq. 6 one can obtain the initial model parameter.

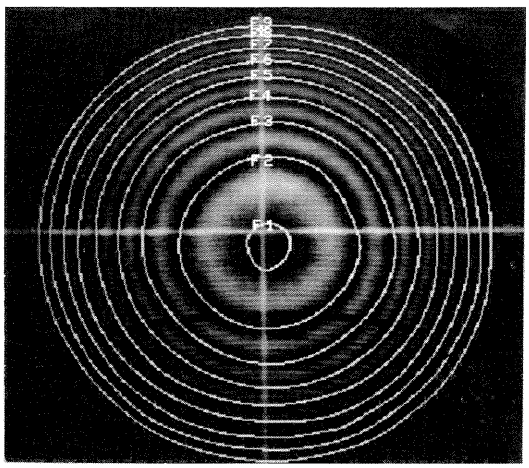

Figure 5. Topogram of Sphere

Input fringe pair	Normalized error for order relationships			Output fringe order
	$n_j < n_i$	$n_j = n_i$	$n_j > n_i$	
$F_j : F_i$				n_1=16.5 n_2=17.5
$F_3 : F_2$	1.0	2.0	2.2	n_3=18.5
$F_4 : F_3$	1.0	2.0	5.6	n_4=19.5
$F_5 : F_4$	1.0	6.0	10.6	n_5=20.5
$F_6 : F_5$	1.0	19.7	30.1	n_6=21.5
$F_7 : F_6$	1.0	7.4	11.5	n_7=22.5
$F_8 : F_7$	1.0	56.3	50.6	n_8=23.5
$F_9 : F_8$	1.0	30.6	29.9	n_9=24.5

Table 1. Analysis of Sphere Topogram

6. Experimental Results

The method described above was embodied into a program to automatically order a set of ordinary moiré fringes. The program was written in Fortran 77 and was run on a commercial image analysis system [2]. The moiré topograms used were of a standard test object designed at NRC (Paulun, 1983) and of a human back from a biomedical application. These topograms were produced using shadow moiré instruments developed in our section (Van Wijk, 1980).

For a given moiré topogram, we first digitize it using a CCD image scanner to put it into computer memory. We then trace out the contours using the digital display and interactive software (an automated tracer is under development as part of a completely automated topogram analysis package). The contours are stored as a sparse series of *turning-points* along the curve. A quadratic spline function is used to reconstruct the plane curves $F(t)$ of each of the so-stored fringe contours in the set as a continous string of connected pixels in the digital image.

At this stage, software to test the fringe ordering principles described above was invoked. It searched from each point in straight line normal to the curve to obtain $L(s)$. Using two initially known fringes as seeds, the program automatically analyzed the rest of the fringes by using the method discussed in Section 5 and reported the ordering result. Figure 5 and Table 1 show the moiré topogram for the spherical test object and the ordering result. Figure 6 and Table 2 show a moiré topogram of a human back and the outcome of that test. In both tests we used $F_1, F_2, \ldots, F_M$ to denote the *dark* fringes and assumed that the fringes F_1 and F_2 are initially known to have fringe number $n_1 = 16.5$ and $n_2 = 17.5$. Then for each indicated neighbouring-fringe pair, the error between the image brightness and the estimated reflectance value for each of three possible order relationships was calculated. The case which produced the minimum error (normalized) was

[2] An ARIES-II from DIPIX Systems, Ltd. (Ottawa)

selected, with the appropriate value of the fringe number assigned so as to be used in the analysis of subsequent pairs. In both examples, the results are *everywhere* consistent with the actual shape of the test objects.

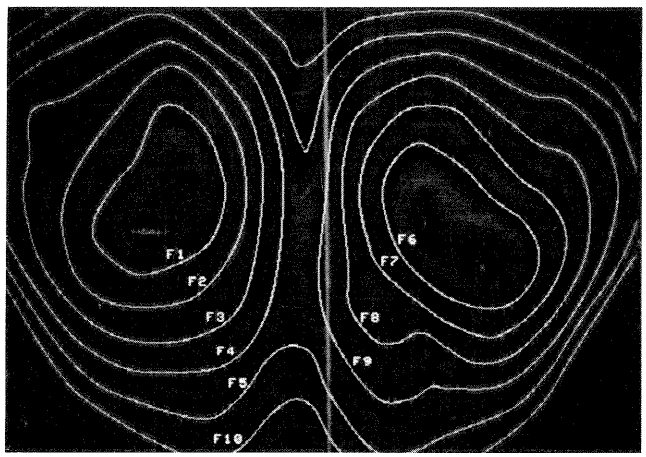

Figure 6. Topogram of Human Back

Input fringe pair	Normalized error for order relationships			Output fringe order
	$n_j < n_i$	$n_j = n_i$	$n_j > n_i$	
$F_j : F_i$				$n_1 = 16.5$ $n_2 = 17.5$
$F_3 : F_2$	1.0	12.8	19.1	$n_3 = 18.5$
$F_4 : F_3$	1.0	5.9	11.1	$n_4 = 19.5$
$F_5 : F_4$	1.0	12.8	20.3	$n_5 = 20.5$
$F_6 : F_7$	17.4	12.1	1.0	$n_6 = 16.5$
$F_7 : F_8$	3.1	3.3	1.0	$n_7 = 17.5$
$F_8 : F_9$	2.3	2.2	1.0	$n_8 = 18.5$
$F_9 : F_5$	2.4	2.1	1.0	$n_9 = 19.5$
$F_{10} : F_5$	1.0	13.4	20.1	$n_{10} = 21.5$

Table 2. Analysis of Back Topogram

7. Concluding Remarks

In this paper we described a method to order ordinary moiré fringes based on the known moiré image formation geometry and a simple photometric model. We presented an algorithm to determine the surface normal at a point by using the vector product of two tangent vectors of the surface curves which intersect at that point. We then described the steps in our method and gave the results of test runs for a standard object and a human back. The normalized errors listed in Tables 2 and 3 clearly show a strong discrimination between the correct case and the other cases. We conclude that photometric analysis can be used to order ordinary moiré fringes.

These results were from a prototype software development. There are several aspects in this method which may need further consideration. For example, the photometric model could include the specular reflection component from the object, instead of assuming a purely diffuse effect. We are investigating various methods to obtain the surface reflectance values in the presence of the moiré patterns. Also, there is a need to seek a more robust algorithm for estimating the photometric model parameter, thereby weakening the constraints on the initial conditions to run the program. Since this writing, some of these issues have been introduced into a more sophisticated version of the software, which will be reported elsewhere (Pekelsky and Ding, 1986).

Acknowledgements

We would like to thank D. Havelock for his helpful assistance and many valuable suggestions. The drawings are from the pen of D. Honegger. The authors also want to thank M. Paulan, H. Ziemann and other members of the Section for their many valuable discussions and encouragement. Ding Xinhong also would like to thank his host, Z. Jaksic, the head of the Photogrammetric Research Section for providing this research opportunity at the NRC.

References

1. Horn, B. K. P., 1975. "Obtaining shape from shading information", *Psychology of Computer Vision* (Edited by P. H. Winston) McGraw-Hill, New York, pp. 115-155.
2. Ikeuchi, K. and B. K. P. Horn, 1981. "Numerical shape from shading and occluding boundaries", *Artifical Intelligence*, Vol. 17, pp. 141-184.
3. Paulan, M., 1983. "A standard object for moiré topography", *Moiré Fringe Topography and Spinal Deformity, proceedings of the 2nd International Symposium* (Edited by B. Drerup, W. Frobin, E. Hierholzer), pp. 233-240. Gustav Fischer Verlag, Stuttgart, New York.
4. Pekelsky, J. R., 1985. "Automated contour ordering in moiré topograms for biostereometrics", SPIE Vol. 602, *4th International Meeting on Biostereometrics*, 2-6 December, Cannes, (in press).
5. Pekelsky, J. R., 1984. "Automated analysis of moiré topograms for the detection and diagnosis of scoliosis", *Surface Topography and Spinal Deformity, Proceedings of the 3rd International Symposium*, 27-28 Sept. Oxford, England, (in press: Gustav Fischer Verlag, Stuttgart, New York, 1985).
6. Pekelsky, J. R. and Ding Xinhong, 1986. "Photometric ordering of moiré fringes", SPIE Vol. 661, *Optical Testing and Metrology*, 3-6 June, Quebec City, (in press).
7. Pentland, A. 1984. "Local Shading Analysis", *IEEE Trans. On Pattern Analysis and Machine Intelligence*, Vol. PAMI-6, No. 2, March, pp. 170-187.
8. Takasaki, H., 1970. "Moiré topography", *Applied Optics*, Vol. 9(6), June, pp. 1467-1472.
9. Van Wijk, M. C. 1980. "Moiré contourgraph – an accuracy analysis", *Journal of Biomechanics*. (GB), Vol. 13(7), pp. 605-613.